DOE Award Number: DE-FG36-08GO18064

Heracles Energy Corporation
d.b.a.
Prometheus Energy

Active Magnetic Regenerative Liquefier

Final Report

PREPARED BY

Prometheus Energy

PROJECT TEAM

John A. Barclay, Principal Investigator
Kathryn Oseen-Senda
Luke Ferguson
Anand Cousins
Jamshid Pouresfandiary
Heather Ralph
Tom Hampton

Submitted January 12, 2016

Table of Contents

1. PROJECT TIMELINE 4

2. PROJECT GOAL AND OBJECTIVES 5

3. SIGNIFICANT RESULTS –AMRR DESIGN 6

3.1. SUPERCONDUCTING (S/C) MAGNET SUBSYSTEM 10
3.2. MECHANICAL SUPPORT STRUCTURE WITH LOW THERMAL LEAKS FOR THE MAGNET 14
3.3. GIFFORD-MCMAHON (GM) CRYOCOOLER SUBSYSTEM FOR THE S/C MAGNET 15
3.4. HIGH VACUUM COLD BOX 15
3.5. INSTRUMENTATION/CONTROLS/DAQ SUBSYSTEM 16
3.6. MAGNETIC REGENERATORS SUBSYSTEM 18
3.7. REGENERATOR DRIVE SYSTEM 19
3.8. HEAT TRANSFER FLUID SYSTEM 21

4. PRELIMINARY EXPERIMENTAL TEST RESULTS 26

5. PROJECT MANAGEMENT AND REPORTING 28

6. COST STATUS 28

7. DESCRIPTION OF ANY PRODUCT PRODUCED OR TECHNOLOGY TRANSFER ACTIVITIES 28

1. Project Timeline

This document is the final report for the DOE Project entitled Active Magnetic Regenerative Liquefier (AMRL) funded under Grant DE-FG36-08GO18064 to Heracles Energy Corporation d.b.a. Prometheus Energy (Prometheus). This final report does not contain any proprietary or personally identifiable information.

In the original Notice of Financial Assistance Award to Prometheus signed by Stephanie Carabajal of the Golden Field Office on July 3, 2008 and by Kirt Montague, our CEO, on July 11, 2008, the original budget period was from June 1, 2008 through September 30, 2009. The original project period was from June 1, 2008 through May 31, 2011. In June 2009 our request to extend the period of budget period 1 from September 30, 2009 through September 30, 2010 was approved. In that award modification the allocated funds for budget period 1 were increased from $676,947 to $1,076,874.

In August 2010 we requested a modification of the award to extend budget period 1 from September 30, 2010 through March 31, 2011 and the authorized funds were increased to $1,576,947. The 20% cost share of the total project funding obligation from Prometheus correspondingly increased to $369,237. The project technical execution date was extended through 5/31/2012.

In January 2011 Prometheus's Board of Directors decided that the company would dissolve its Advanced Technology Group on May 31, 2011. The Board asked John Barclay, the Chief Technology Officer of the company and the Principal Investigator on the AMRL project, to form a new energy company into which the technology could be transferred.

All professional staff executing the AMRL project left Prometheus in mid-2011. On May 31, 2011 all technical project work was put on hold but the award was maintained until June 30, 2014 through no-cost extensions.

John Barclay co-founded Emerald Energy NW, LLC (EENW). On November 9, 2012 with the DOE approval Prometheus and EENW executed the Assignment and Assumption Agreement for the DOE Award # DE-FG36-08GO18064. However, the award transfer completion was contingent on securing sufficient funding by EENW to complete the project. Unfortunately, as of June 2014 EENW was unable to secure sufficient funds and the award was officially terminated on June 30, 2014.

On October 23, 2014 all AMRL equipment was shipped from the storage facility in Kirkland, WA to the Pacific Northwest National Laboratory (PNNL) Energy and Environment Directorate in Richland, WA. In October 2014 Prometheus submitted all documents related to the AMRL property transfer to PNNL.

Prometheus filed 12 quarterly (Q3 2008 – Q2 2011) and 3 annual (2009 -2011) technical progress reports.

2. Project Goal and Objectives

The primary goal of this project was to make significant technical advances toward highly efficient liquefaction of hydrogen.

Conventional hydrogen liquefiers at any scale have a maximum FOM of ~0.35 due primarily to the intrinsic difficulty of rapid, efficient compression of either hydrogen or helium working gases (depending on the liquefier design). The novel approach of this AMRL project uses solid magnetic working refrigerants cycled in and out of high magnetic fields to execute an efficient active regenerative magnetic liquefaction cycle that avoids the use of gas compressors.

AMRL technology promises cost-effective and efficient liquefaction of hydrogen because it eliminates the compressors, the largest source of inefficiency in Claude cycle liquefiers. However, as with any innovative technique, many questions have to be investigated and understood before commercial applications happen. Since the mid-1970s, magnetic refrigeration technology for applications above 1 K beyond research laboratory use has been investigated with increasing understanding of magnetic cycles, magnetic refrigerants from ~4 K to ~300 K, and practical magnetic refrigeration prototype designs. The seminal patent on the 'active magnetic regenerator' was issued in 1982. The principle of operation this unique refrigeration cycle is illustrated as an Active Magnetic Regenerative Refrigerator (AMRR) in Figure 1. Only in the last ~15-20 years have there been significant engineering efforts on two commercial applications of magnetic refrigeration: those with small cooling power (~100 W), non-chlorofluorocarbon refrigeration near room temperature using permanent magnets and much larger capacity cryogenic liquefiers for hydrogen and natural gas (~100s of kW of refrigeration).

The AMRL project funded under this DOE award was an extensive engineering effort to analyze, design, fabricate, and test innovative natural gas and hydrogen liquefier prototypes. Successful demonstration of AMRL prototypes will answer a few key design questions and provide a proven knowledge base to enable use of advanced liquefiers for various hydrogen infrastructure projects that cost-effectively provide liquid hydrogen (LH2) energy storage/delivery for gaseous hydrogen produced by several sources including electrolysis at intermittent wind or solar energy plants. The AMRL technology readily scales up or down in capacity so it could be scaled to reach DOE's target of 30 te/day and down to a vehicular refueling station size of ~2-3 te/day where gaseous hydrogen continuously produced via steam methane reformation, or high temperature fuel cells, or electrolysis could be liquefied, stored and supplied as LH2 and/or compressed hydrogen produced from liquid hydrogen (LCH2).

Numerical simulation modeling of high performance AMRL designs indicates certain achievable designs have promise to simultaneously lower installed capital costs/unit capacity and to increase thermodynamic efficiency from a FOM of ~0.35 toward ~0.5 to ~0.6. Results from experimental prototypes should support the design and deployment of hydrogen liquefier plants that meet the DOE hydrogen production and delivery targets:

- Delivery cost of LH_2 at <$1.00/kg
- $40 MM capital cost for a turn-key plant with a capacity of 30 te/day
- Operational efficiency of a complete liquefier plant of 75% as defined by DOE and commensurate with a liquefier FOM of ~0.6.

To achieve the primary goals of this project our objectives were to model, design, build, test and demonstrate two devices; a single-stage active magnetic regenerative refrigerator (AMRR) spanning from ~290 K to ~120 K as the first lab prototype and an engineering-scale active magnetic regenerative liquefier (AMRL) for ~25 kg/day of hydrogen incorporating knowledge gained from the lab-scale prototype. The AMR Refrigerator and Liquefier modules are the key modules of a complete LH_2 facility. A typical block process flow diagram for a LH_2 facility using AMRL technology is shown below.

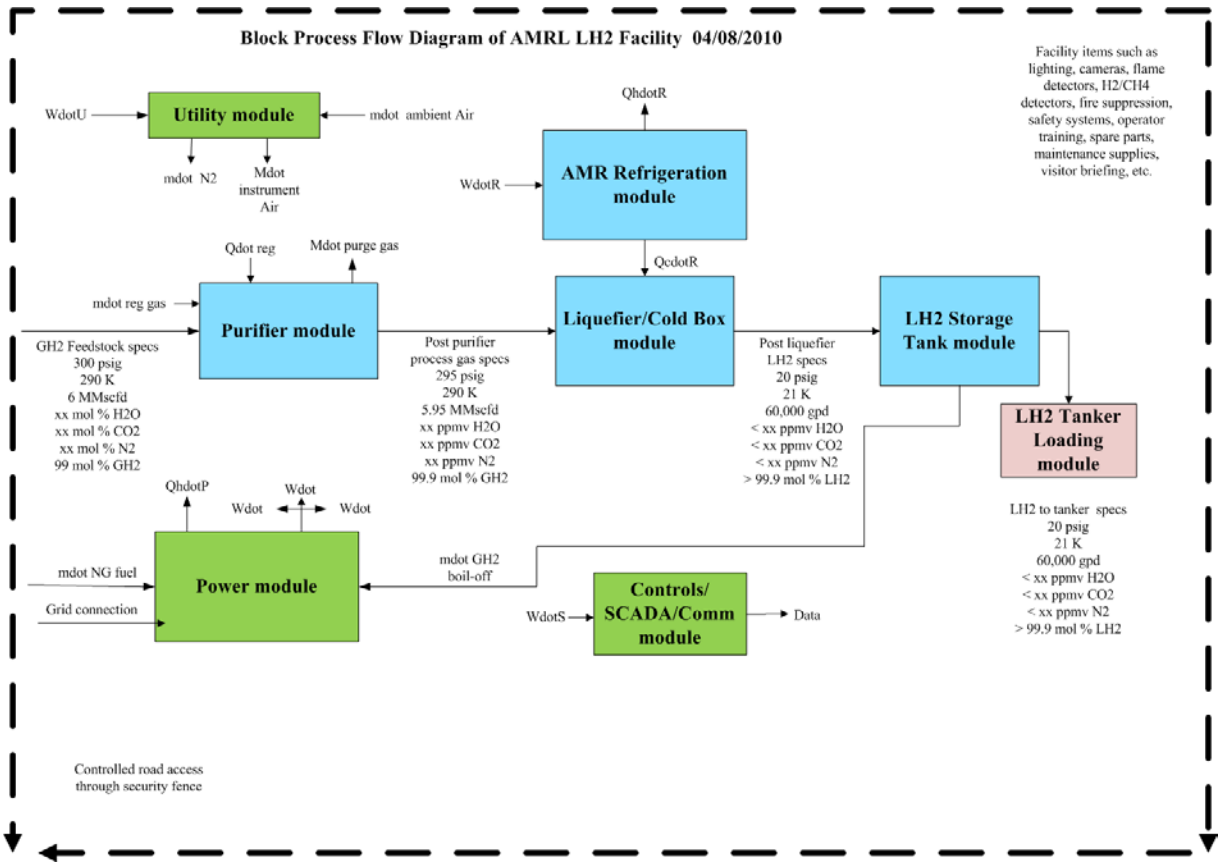

Figure 1. A Block Process Flow Diagram of the AMRL showing purifier systems, liquefier systems, other plant systems, and safety and security components of a complete facility.

Discussion of magnetic refrigeration principles underlying this project can be found in the final report for the DOE SBIR Phase I Project entitled Active Magnetic Regenerative Liquefier funded under Grant DE-FG02-07ER84783 and submitted by Prometheus in April 2009. The design basis for the first lab-scale prototype AMRR operating between ~290 K and ~120 K was to be established in concert with the overall system design and predicted performance characteristics using the detailed active magnetic regenerative refrigerator numerical simulation model developed during the Phase I SBIR award.

3. Significant Results –AMRR Design

The Prometheus project team designed, built, and tested eight subsystems for a single-stage active magnetic regenerative refrigerator (AMRR):

1. Superconducting (s/c) magnet subsystem,
2. Mechanical support structure with low thermal leaks for the s/c magnet,
3. Gifford-McMahon (GM) cryocooler subsystem for the s/c magnet (for conduction cooling of thermal shield and s/c magnet),
4. High vacuum cold box,
5. Instrumentation/controls/DAQ subsystem,
6. Magnetic regenerators subsystem,
7. Regenerator drive system, and
8. Heat transfer fluid system.

The last three subsystems (6-8) of the AMRR prototype were completed and integrated near the end of the first quarter of 2011. This successfully integrated AMRR prototype was described in the poster presented at the Annual Merit Review of DOE's Hydrogen Production & Delivery programs in May 2011. Preliminary integrated system shake-down experiments and initial cooling tests were carried out in the second quarter of 2011, just before the project was suspended on May, 31 2011.

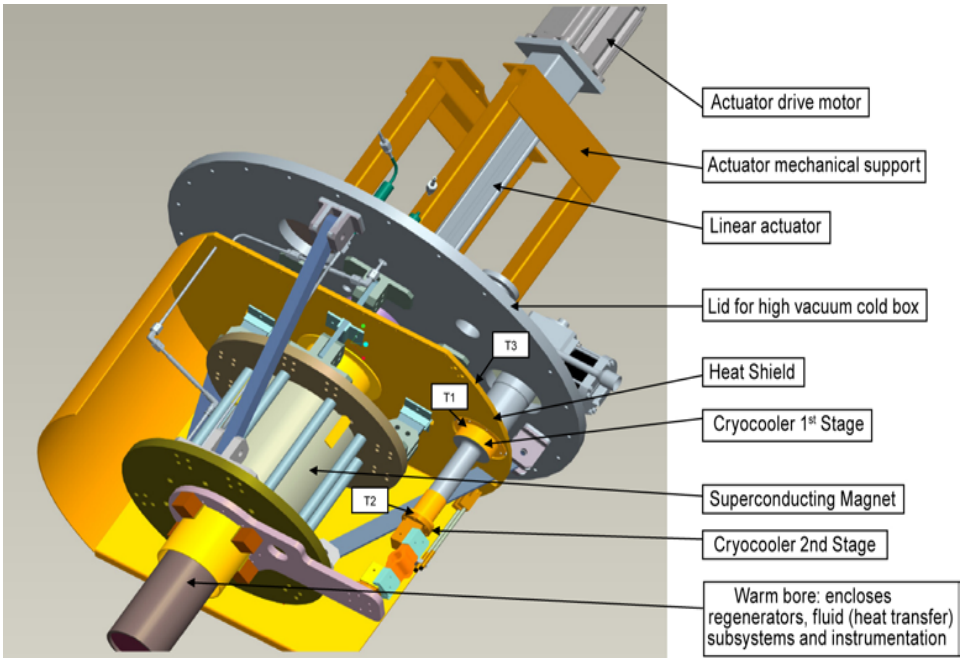

Figure 2. Three-dimensional reciprocating AMRR prototype design.

The completed three-dimensional mechanical design of the first laboratory-scale AMRR prototype with dual regenerators reciprocating in and out of a 7 Tesla (T), large bore superconducting magnet is illustrated in Figure 2 and Figure 3. It includes the various components of the eight subsystems required to execute the AMRR cycle. This prototype is designed to operate between ~290 K at the hot end and cold end temperatures down to as low as ~120 K. The design required numerous calculations of the thermodynamics, heat transfer, fluid dynamics, structural loads, and many related items. One of the more challenging design features was the support of the 4 K superconducting magnet that has to be structurally capable of

withstanding large magnetic forces between the magnetic materials in the dual regenerators and the magnetic field of the magnet. The center access tube (warm bore in Figure 2) through the magnet is insulated from the magnet to enable the dual regenerators to operate between ~290 K and ~120 K. Figure 3 shows a mechanical design of the prototype that includes the superconducting magnet, the Gifford-McMahon (GM) cryocooler to conduction cool the magnet and thermal shield, the elaborate support structure, and the top plate to mount the prototype in the double-walled Dewar that serves as the cold box.

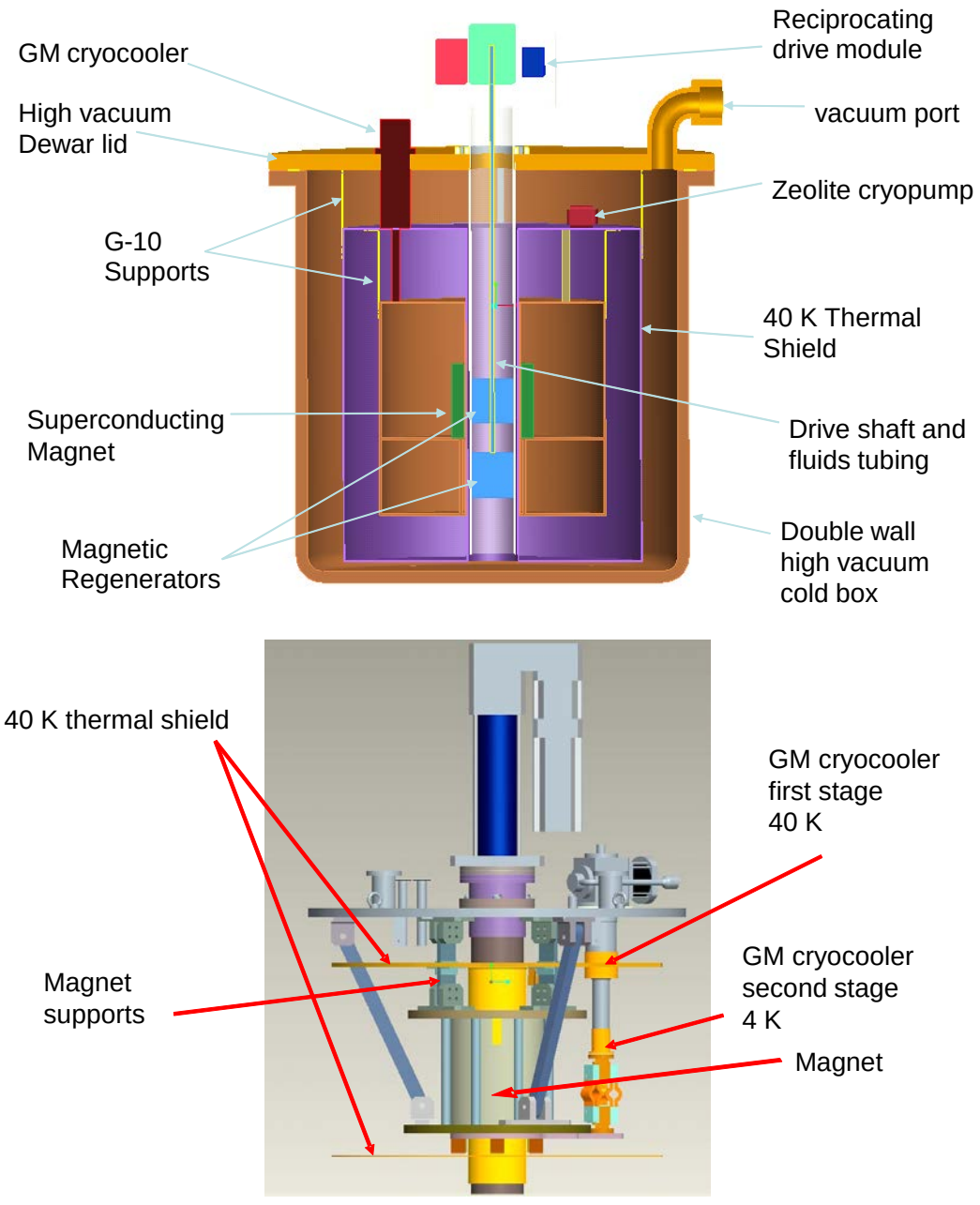

Figure 3. Mechanical design of the 290 K to 120 K AMRR prototype: cold box cross-section (top) and details of the mechanical suspension system for the magnet (bottom).

Figure 4 shows a photograph of the partially assembled AMRR prototype with the bottom heat shield ready to be raised and attached to the ~40 K thermal shield. The prototype has been instrumented with numerous sensors and connected to a LabVIEW-based data acquisition system. The cold box was evacuated to ~1 x 10^{-7} torr for excellent thermal isolation from the surroundings. The GM cryocooler (Sumitomo Heavy Industries, model 415D) cooling power was measured and found to be better than the manufacturer's specifications (1.5 W of cooling at 4.2 K and 40 W of cooling at 60 K).

The GM cryocooler successfully cooled the magnet before it was charged with a proper power supply designed for high current, low voltage and operated in persistent mode. The magnetic field profile was measured as was the adiabatic temperature change in a sample of gadolinium (Gd). Both of these measurements gave results that agree very well with calculated values.

Figure 4. Photograph of the AMRR system before insertion in the cold box.

The following sections provide additional information about all eight major subsystems of the ARRR prototype built by Prometheus.

3.1. Superconducting (s/c) magnet subsystem

We considered three different superconducting magnet geometries; a partial tokamak, a dipole, and a solenoid. These choices are coupled to the design of the magnetic regenerator. For the cylindrical regenerator geometry the lowest risk and least expensive choice for the superconducting magnet is a simple solenoid. This choice dictates the selection of the drive mechanism because either the magnetic regenerators have to move or the superconducting magnet has to move. We chose to move the regenerators.

The superconducting magnet was purchased from Cryomagnetics, Inc. of Oak Ridge, Tennessee along with integrated quench protection, temperature sensors, a persistent mode switch, high temperature superconducting leads and a superconducting-magnet-specific power supply. Cryomagnetics sent us detailed magnet design drawings for incorporation into our mechanical model. The exact dimensions of the magnet have been incorporated into our magnetic field and force calculations.

The large-bore superconducting magnet with a maximum field of 7 T that is thermally shielded by an OFHC copper shield held at ~50 K and supported by crossed braces from the Dewar (cold box) lid. The magnet and other subsystems of the AMRR are enclosed in a Dewar evacuated to ~1 x 10^{-7} torr. The thermally shielded cylindrical bore required to separate the cold magnet from the warmer regenerators is part of this vacuum space to reduce any convective heat transfer to a negligible value. The pair of magnetic regenerators mounted on a common axis is moved in and out of the magnetic field and the forces have been balanced to the maximum extent possible.

The initial thermal design of the magnet subsystem including convective, conductive and radiative heat leaks to the magnet (at ~4 K) and shield (at ~40 K) was done in Mathcad to be adaptable to changes dictated by the magnetic or structural requirements. More detailed 3-D thermal simulations were done in the heat transfer module of COMSOL and are similarly flexible.

The structural subsystem mechanical design of a reciprocating design of a 290 K to 120 K AMRR prototype required numerous calculations of heat transfer, fluid dynamics, structural loads, and many related items. One of the more challenging design features was the support of the 4 K superconducting magnet that has to be structurally capable of withstanding large magnetic forces between the magnetic materials in the regenerators and the magnetic field of the magnet. The large magnetic forces impact the design of mechanical drive mechanism; i.e., an AMRR cycle takes ~0.1 seconds to magnetize/demagnetize by moving the dual regenerators ~26 cm along the vertical z axis of the s/c magnet solenoid. The regenerators stop for dwell periods of ~0.5 seconds while the heat transfer fluid flows from hot to cold or cold to hot through the regenerators.

The temperature distribution around the thermal shield was analyzed using conduction and radiation heat leaks with, oxygen-free, high conductivity (OFHC) copper sheet. The conduction

connections between the cryocooler and the support members at several locations on the thermal shield were carefully modeled to ensure there were no significant temperature gradients for the various heat loads expected. Numerous temperature sensors were attached to the shield to verify these calculations. The various components of the thermal shield were manufactured in-house.

Detailed magnetic field and force calculations were done using the AC/DC module of COMSOL Multiphysics code. The 2D axisymmetric and 3D forces between the magnet and magnetic regenerators were calculated using Maxwell's equations with magnetic permeability chosen for gadolinium (Gd). The magnetic force calculations couple the magnetic regenerator subsystem, structural magnetic force subsystem, and the drive subsystem. Detailed calculations of the magnetic field distribution in the presence of the magnetic regenerators and the associated magnetic forces are essential to the overall design. We have studied multiple design choices to best balance the magnetic forces of the two regenerators and the magnet as the regenerators are reciprocally moved during the magnetic cycle. One of the magnetic regenerators is located in center of the magnet and the second one is located on the central axis above or below the magnet. The requirement to have the demagnetized regenerator in a net magnetic induction of ~0.1 T while the magnetized regenerator is at the maximum induction of ~7 T determines the minimum separation between the two regenerators and the stroke length of the axial motion for the cycle.

This separation produces an unfortunate feature of an axially reciprocating AMRR design, i.e., the net balanced magnetic forces are much larger than those required for the magnetic cycle alone. Using magnetically soft iron (Fe) support structure between the two identical magnetic regenerators and on the drive mechanism, it is possible to reduce the force imbalance somewhat but our detailed 3-D calculations show (see Figure 5) it is impossible to reduce the net forces close to those required for the AMRR cycle. This large intrinsic force imbalance has significant implications on the drive subsystem and the structural support subsystem.

Calculated magnetic forces on a single gadolinium cylindrical regenerator with ~5" outer diameter and ~5" length at 7 Tesla are shown in Figure 5. The same figure (bottom graph) includes the force reduction that is possible when two identical magnetic regenerators are balanced as much as possible. This force imbalance is several times larger than the net magnetic force required to provide the work input for the thermodynamic cycle and suggests a future rotary rather that reciprocating AMRL choice.

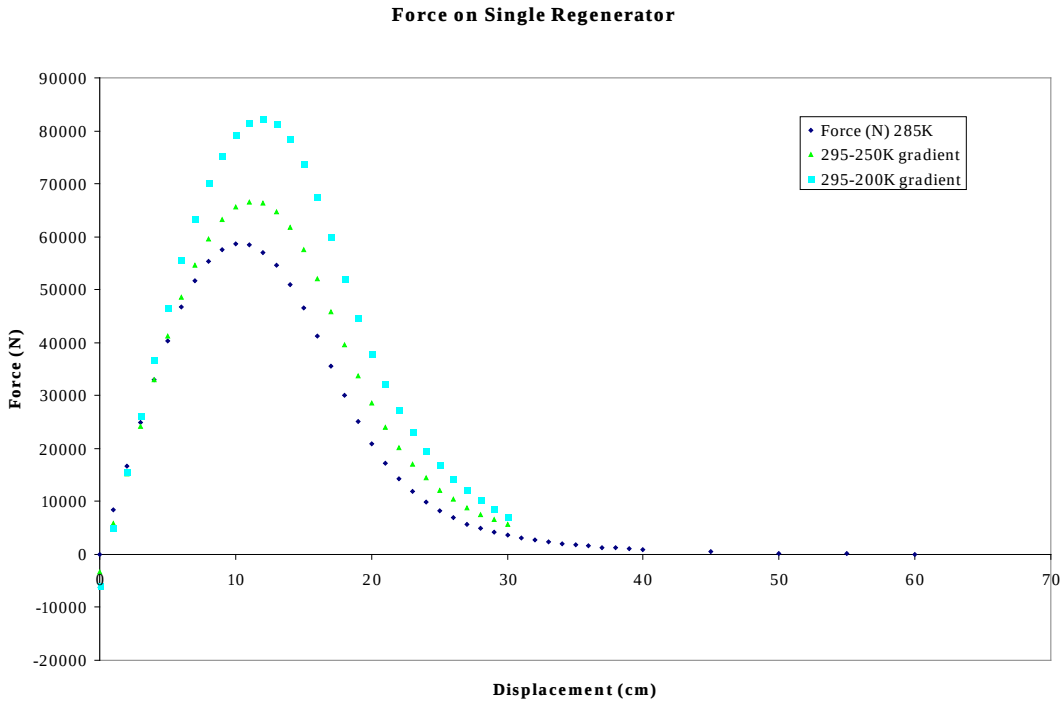

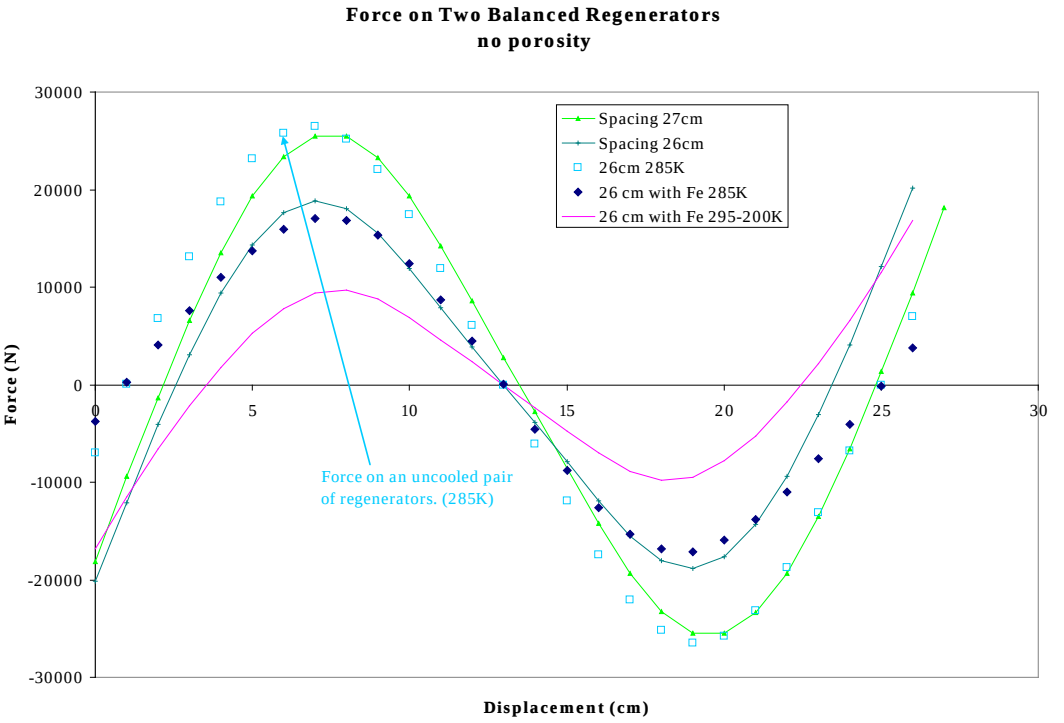

Figure 5. Calculation of magnetic forces between s/c magnet and magnetic regenerators

The AC/DC module of the COMSOL Multiphysics code was used to calculate the 3-D magnetic field profile and magnetic forces on the dual magnetic regenerators (assuming Gd permeability).

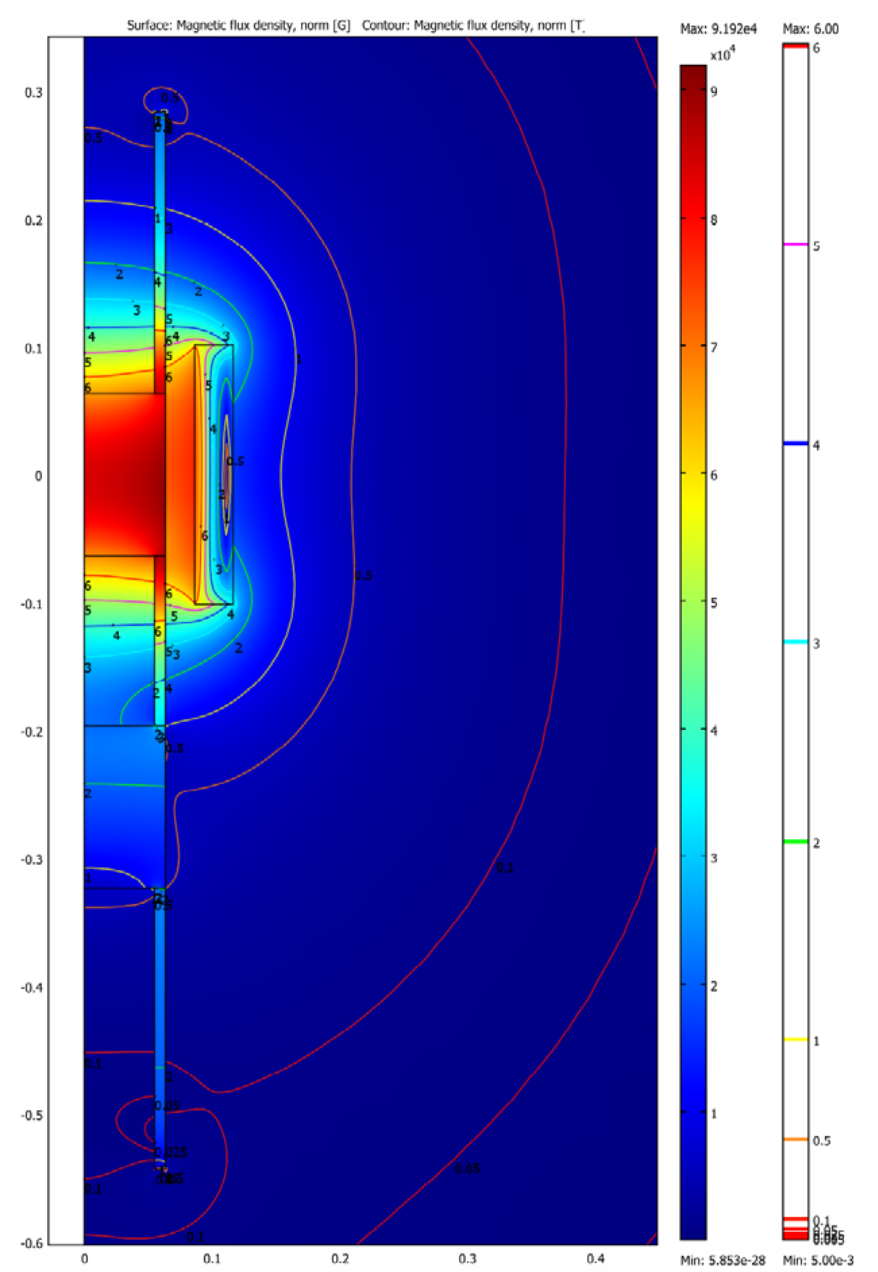

Figure 6. Magnetic flux density profile for the AMRR design

Figure 6 shows a color contour of the magnetic flux density of the cylindrically symmetric superconducting winding in the presence of two cylindrical magnetic regenerators located on the central axis of this figure. It also shows the superconducting winding in outline. One of the dual regenerators is located in the center of the magnet and the second one is located below the magnet. The thin Fe support cylindrical ring is shown extending above, between, and below the dual magnetic regenerators.

3.2. Mechanical support structure with low thermal leaks for the magnet

After analyzing several configurations of magnet supports to the top of the magnet form and the bottom of the magnet form, a workable configuration was selected. This subsystem was custom fabricated and the assembled structure is very robust.

The structural subsystem in the cold box needs to support both the superconducting magnet and the thermal shield at ~40 K. In addition it needs to be strong enough to react the large magnetic forces between the magnetic regenerators and the superconducting magnet. The magnetic regenerators have a temperature gradient along them ranging from ~290 K at the hot end to ~120 K at the cold end while the magnet has to be cooled to ~4 K to operate. The structure has to support the following loads:

- Calculated peak magnetic force: 1.92 x 104 N (~4,315 lbf)
- Weight of magnet from the manufactured specifications: ~981 N (~220 lbf);
- Estimated weight of thermal shield: ~934 N (~210 lbf).

The support structure has to simultaneously provide excellent thermal isolation of the thermal shield at ~40 K and the magnet at ~4 K. The selected support design (see Figure 3) has vertical G-10 members from the top of the magnet at ~4 K to the thermal shield at ~40 K and it has diagonal G-10 supports from thermal shield to the bottom of the magnet. There are vertical G-10 supports pinned within stainless steel brackets from the inside bottom side of the Dewar lid at ~290 K to the thermal shield at ~40 K. The support structure is additionally strengthened by transverse G-10 bars at 45 degree angles from bottom of the magnet at ~4 K to Dewar lid at ~290 K to react any horizontal loads caused by the reciprocating motion of the dual axially-separated regenerators. The magnet is held captive by addition two circular rings mounting the magnet as a sandwich by four connecting stainless steel bolts outside the magnet along magnet axis.

The safety factor chosen was a factor of two for the overall support structure and four for a few special parts such as shear in threads. The proper materials for the supports and the connections were chosen to operate at temperature near 4 K and have as little conductive heat transfer as possible. Calculations using Mathcad based on validated data for different materials quantified the conduction heat transfer from three different types of aforementioned vertical and inclined supports for G-10 fiberglass, and 304L stainless steel with existing commercial sizes of solid bars and rectangular tubes. The resultant heat leaks are:

- Conduction heat transfer to magnet is ~0.221 W through the upper support members and ~0.110 W through the bottom support members when the magnet is at 4 K for a total calculated heat leak rate of ~0.331 W. This is well below the cooling power of the 2nd stage of the GM cryocooler of ~1.5W at 4 K.
- Conduction heat transfer to thermal shield is ~3.223 W through the upper support members and ~2.944W through the bottom support members for a total heat leak to the shield of ~6.167 W. This is well below the cooling power of the 1st stage of the GM cryocooler of ~50 W at ~40 K.

3.3. Gifford-McMahon (GM) Cryocooler Subsystem for the S/C Magnet

The superconducting magnet is operated at ~4 K. The cooling required to keep the magnet at ~4 K was accomplished by using conduction cooling from a two-stage GM cryocooler rather than using liquid helium and liquid nitrogen.

The two-stage GM cryocooler (made by Sumitomo Heavy Industries, model 415D) used to the superconducting magnet to ~4 K was integrated with the structural support subsystem for the magnet. It includes the coupling to the thermal shield that is used to intercept heat leaks at ~40 K. The second stage of the cryocooler is connected to the superconducting magnet via a highly conductive flexible coupling.

The GM cryocooler uses high purity He gas as its refrigerant. The high pressure of ~300 psia is provided by a scroll compressor with an input power of ~7.5 kW. The suction pressure of the expanded He gas enters the compressor at ~50 psia. The high purity He gas refrigerant was purged twice after the initial cool down experiments. A set of experiments to calibrate numerous temperature sensors and to measure the load map of the cryocooler was done. The thermal load map of the cryocooler measured was better than that specified by the vendor with an ultimate temperature of ~2.6 K on the second stage and slightly over 1.5 W of cooling at 4 K.

3.4. High Vacuum Cold Box

The cold box isolates the cryogenic parts of the prototype from ambient conditions. This was accomplished very effectively with a double-walled vacuum insulated Dewar. A stainless steel lid with numerous welded feedthroughs seals all the penetrations into the cold box (see Figure 7). All the subsystems are mounted from the lid so the entire prototype can be inserted or removed by lifting the top lid. After the lid is sealed to the Dewar the cold box is evacuated with a turbo-molecular pump. This condition thermally isolates the various components of the AMRR prototype from each other. The original cold box lid had to be substantially modified to accommodate the requirements of the structural support subsystem and the central tube for the reciprocating magnetic regenerator subsystem. The mechanical drawings for all the changes were made and a qualified local machine shop with welding capabilities was used to make the changes.

There was some warpage to the lid as the several holes were cut and/or weldments made. This complicated the vacuum sealing of the lid to the Dewar but this was overcome with a larger O-ring and closely-spaced bolts. In future lid designs, a transverse stainless steel brace pattern will be welded onto the lid before cutting holes and making various weldments to minimize the warpage. All the subsystems are mounted from the lid so the entire prototype can be inserted or removed from the Dewar by lifting the top lid. After leak checking with a He mass spectrometer detector, the Dewar cold box was evacuated with a turbo-molecular pump to a high vacuum pressure of ~1 x 10^{-6} torr. We have also added a zeolite-filled adsorption porous cylinder to the 1st stage of the GM cryocooler to provide a high capacity cryopump during cool down and operation. This enables the turbo-molecular pump to be isolated from the Dewar and turned off once cool-down begins. The vacuum in the Dewar is ~1 x 10^{-7} torr which provides excellent convective thermal isolation in the AMRR prototype.

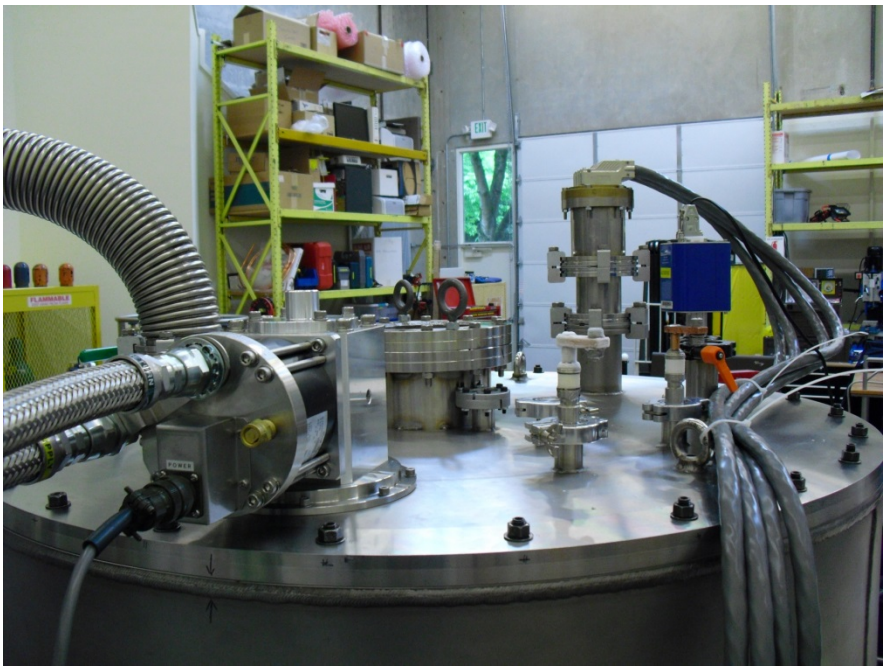

Figure 7. Cold box lid

3.5. Instrumentation/Controls/DAQ Subsystem

The temperatures, pressures, flow rates, magnetic field, operating frequency, and powers must be measured in numerous locations to fully characterize the operation of the first AMRR prototype.

We purchased numerous sensors to test the AMRL. Most of the flow and pressure transducers were calibrated at the vendor's facilities. A few factory-calibrated temperature sensors (Cernox^{TM}) were purchased. These were being used to calibrate numerous Cu-constantan thermocouples, platinum resistance thermometers (PRTs), and bismuth ruthenium oxide thermometers (ROXTM). We selected several types of temperature sensors that will function well in high magnetic fields and at cryogenic temperatures.
To calibrate numerous temperature sensors against a factory-calibrated Cernox^{TM} sensor with good sensitivity from ~2 K to ~330 K, we designed and built an isothermal block of high conductivity copper (Cu) that was bolted to the 2nd stage of the GM cryocooler with a thin layer of Apezon N grease to ensure good thermal contact. This Cu block has holes or taps to insert or attach different types of sensor and properly heat sink their electrical leads. A common precision current generator was used to supply 10 μA while two voltage leads enable high precision 4-wire measurements of the resistive thermometers to be made. The thermocouple leads were heat sunk before bringing them to the reference junction in the FieldPoint modules at room temperature. The calibrated sensor was checked by using ice bath and LN2 and found to be both accurate and precise. A small heater was attached to the block to enable the temperature to be varied during the calibration process. The pressure, mass flow, and magnetic field sensors were all factory calibrated. All calibration curves or interpolation tables were entered into the LabVIEW program

to present temperatures directly on the GUI screen for the test engineers. All the raw data are saved on the hard disk of the LabVIEW computer for later data reduction and archival.

These temperature sensors and other pressure, flow, magnetic field, and displacement sensors are interfaced via the FieldPoint modules to the LabVIEW DAQ subsystem. The data rates for the tests of the cryocooler and superconducting magnet subsystems can be handled with the FieldPoint modules. However, the rates of data acquisition during an AMRR cycle with the dual regenerators at ~1 Hz are too high for the FieldPoint modules. We will replace these modules with much higher speed Compaq DAQ modules for the LabVIEW program in May. The LabVIEW DAQ and control programs have been successfully tested although there were numerous electrical noise issues that had to be overcome. Our test engineers did an excellent job of diagnosing and overcoming these issues to measure data with excellent precision.

Our objectives were to measure the temperature of magnetic refrigerant throughout the regenerators, the temperature of the heat transfer fluid in several key locations, the pressure of the heat transfer fluid in several locations, the flow rate of the heat transfer fluid, and the position of the magnetic regenerators relative to the center of the solenoidal magnet. Each of these variables needs to be measured sufficiently rapidly to provide detailed temporal resolution during the AMRR cycle which has a period ranging from ~1-2 seconds. The input sampling rate on each sensor is limited by the response time of the particular sensor. For example, the thermocouples have a sample rate of ~50 S/sec. The other variable sensors have faster response times and provide sampling rates of ~100 S/sec or higher. Thus, during a 1 second period for an AMRR cycle, we can only measure the temperatures every 20 milliseconds so a sampling module capable of ~75 S/sec will work fine. The P, flow rate, and position sensors have analog signals with response times of ~100 S/sec so the conversion modules selected have conversion rates of ~1000 S/sec.

The expanded data acquisition system is built around the National Instruments cDAQ-9178 chassis, and is capable of measuring a broad range of analog and digital I/O signals using a high speed USB 2.0 interface. The cDAQ-9178 is capable of output transmission rates of up to 6.4 MS (mega samples)/sec (multi-channel, aggregate) however this rate is dependent on the inputs from the sensors which depends on the type of input module that is installed in the chassis. For example, the maximum sample rate for the 16 channel, 24 bit NI-9213 thermocouple module is 75 S/sec aggregate for all channels. Other modules such as the NI-9219 Universal Analog Input are capable of sample rates of up to 100 S/sec (simultaneous, all channels), and will be used with pressure, flow, and position sensors that are capable of equally high sampling rates (1000 to 100 S/sec). The minimum resolvable time dependence of the pressure and flow rates is expected to be on the order of 10 milliseconds on each input channel, compared with an overall AMRL cycle rate of about 1 Hz.

Our efforts centered on designing and constructing accurate and fast responding temperature sensors that can be used in conjunction with the new high performance cDAQ-9178 based system. An analysis of all the specific requirements (including high immunity to very large magnetic fields, induced noise, fast response times, and restricted space) ultimately lead to the selection of fine-wire cryogenic thermocouples as the best choice for the most critical temperature measurements. A comparison of manufacturer's specifications and published literature showed that the fastest response times for commercially available fine wire (0.001 inch

diameter, butt-welded) thermocouples is about 0.003 seconds, or about 0.015 seconds to reach an accuracy of 99.3% (after 5 time constants). Other considerations, such as mechanical reliability or manufacturability may require larger wire diameters and slower response times; however the NI-9213 sample rate of 75S/s should be adequate for even the fastest 0.001 inch diameter thermocouples.

The new cDAQ-9178 based system will also be used to control and synchronize the motion of the magnetic regenerator assemblies and the heat transfer fluid displacer. Parker C3 ServoManager motion profiles and NI LabVIEW software programs have been successfully developed to test the operation of the linear actuator drive for the magnetic regenerator, and similar motion profiles will be developed for the Copley CME 2 actuator that drives the fluid displacer. Existing LabVIEW control software will be expanded and used to synchronization and optimize motion of both actuator components.

The DAQ subsystem upgrades were successfully integrated into our LabVIEW DAQ subsystem. The programming was perfected during the testing of the linear actuators for the magnetic regenerator drive and the heat transfer fluid piston pump drive. The fabrication and assembly of the three remaining subsystems is progressing well. As they are completed they are being integrated into the AMRR prototype in preparation for initial operational tests of the complete AMRR.

3.6. Magnetic Regenerators Subsystem

We selected Gd spheres as the initial regenerator material because this material is readily available and can span from ~30 K to ~50 K axially along each regenerator with selected, fixed, hot sink temperatures of between ~270 K to ~300 K. For example, if we fix the hot sink temperature at ~280 K, and cycle the AMRR magnetic regenerators in and out of the s/c magnet, we anticipated the cold end of each magnetic regenerator will cool to between ~250 K and ~230 K, depending upon the external thermal load that is applied and the amount of bypass flow of the HTF. A sequence of experiments with the dual, identical Gd regenerators with variable hot sink temperatures and variable cold temperatures for particular AMRR cycle conditions was designed to provide good thermodynamic data to analyze to obtain thermodynamic performance of the AMRR prototype. During assembly of the regenerators the mass of ~100 micron Gd spheres for each regenerator was precisely weighed to ensure that both regenerators were closely matched. After packing the spheres, the pressure drop of the He heat transfer fluid flow through each regenerator was independently measured as a function of mass flow rate for He. This was done before and after each regenerator was impregnated with an alcohol-diluted Stycast 1266 epoxy to bond the spheres into a monolithic, porous bed. The four sets of pressure drop measurements indicated: 1) that the pressure drops were very close to the predicted values using the MacDonald-Ergun equation for pressure drop in porous beds; 2) that the cured epoxy did not block the tiny flow channels in the packed bed; and 3) that the two regenerators were extremely well matched. The installation of several tiny sensors to measure the temperature and flow variables in this subsystem was also successfully completed.

The dual magnetic regenerators must be strong enough to react large magnetic forces and simultaneously be integrated with the pneumatically actuated mechanical drive mechanism and the helium heat transfer fluid subsystem pressurized to ~250 psia. The heat transfer fluid couples the heating and cooling of the magnetic regenerators to the hot heat sink and the cold heat exchanger between the dual regenerators. Figure 8 illustrates the resultant design of the two identical magnetic regenerators and the heat transfer fluid piping including the path for controlled bypass flow of the cold helium heat transfer fluid. Numerous sensors to measure temperature, helium flow rates, magnetic field strength, etc. are also integrated into these subsystems during the fabrication steps. All these sensors had to have vacuum-tight seals to insure that the high pressure helium did not leak into the high vacuum within the cold box during the AMRR operation. These sensors had to operate at high enough frequency to provide time resolution throughout the entire AMRR cycle. They were connected through high speed modules of a Compact-DAQ LabVIEW control and data acquisition computer.

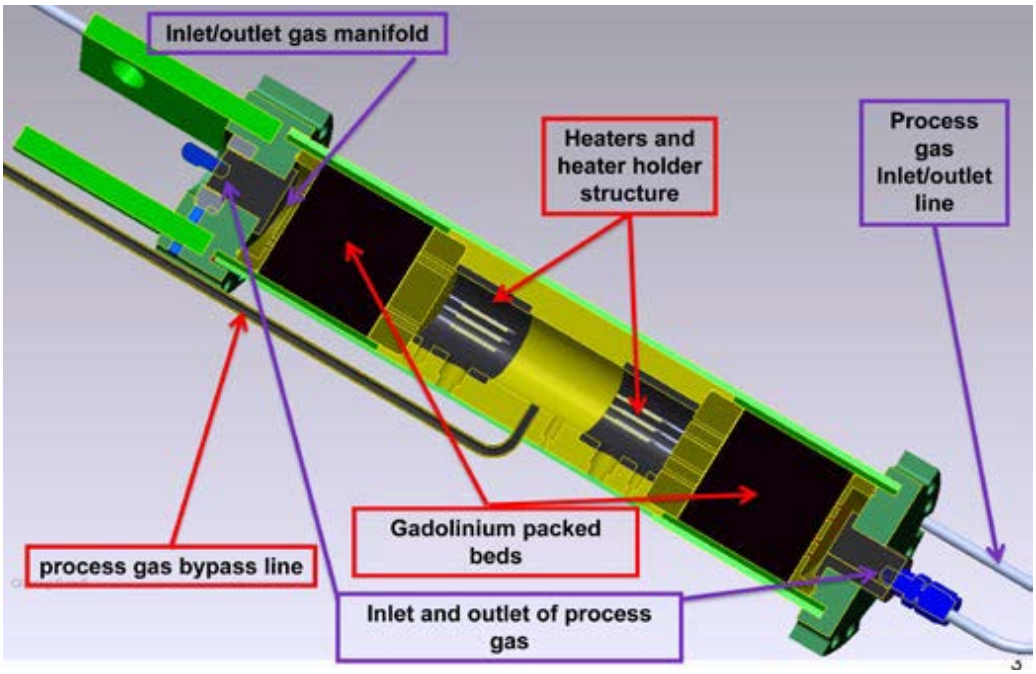

Figure 8. Dual magnetic regenerator design integrates numerous subsystems.

3.7. Regenerator Drive System

The magnetic regenerators are to be moved while the superconducting magnet remains stationary in the 1st AMRR prototype. This arrangement is a change from the original design concept wherein we anticipated moving the superconducting magnet instead of the dual magnetic regenerators. The drive subsystem was also to be designed and built in this subtask.

The linear drive subsystem for the 290 K to 120 K AMRL has presented some requirements that push the envelope of what is commercially available.

Several different drive mechanisms were considered (including pneumatic, hydraulic, bell crank, and ball screw), but because of the limiting factors of our operating environment, required force, and required speed, we chose a ball-screw actuator.

The ball-screw actuator for the magnetic regenerators was assembled and tested using LabVIEW to control the reciprocating motion to execute the AMRR cycle. The drive controller program was written in LabVIEW and successfully used to test the desired motion of the actuator. The programmed regenerator drive motion is trapezoidal in time to meet the requirements for the AMRR cycle (see Figure 11). This particular actuator model uses 480v/3φ power to provide the energy for the hundreds of Newtons of force required to move the magnetic regenerators during the AMRR cycle. The maximum stroke of the drive is reached in a fraction of a second, nominally 0.25 seconds. An equilibrium position is held until the next LabVIEW command to reverse the motion is executed. A passive load was applied to the actuator drive to simulate the magnetic forces on the regenerators during the AMRR cycle.

The pneumatically actuated mechanical drives for the dual magnetic regenerators worked very well after we figured out how to reduce friction and handle the force imbalance as the magnetic field was increased. Figure 10 show the assembled linear actuator in the test configuration.

Figure 10. A picture of the programmable, reversing ball-screw linear actuator for the magnetic regenerator drive subsystem. This actuator is on the test stand in this picture. It is mounted on top of the cold box lid during AMRR operation. One of the two yellow cables is the electrical power cable and the other one is the controls cable.

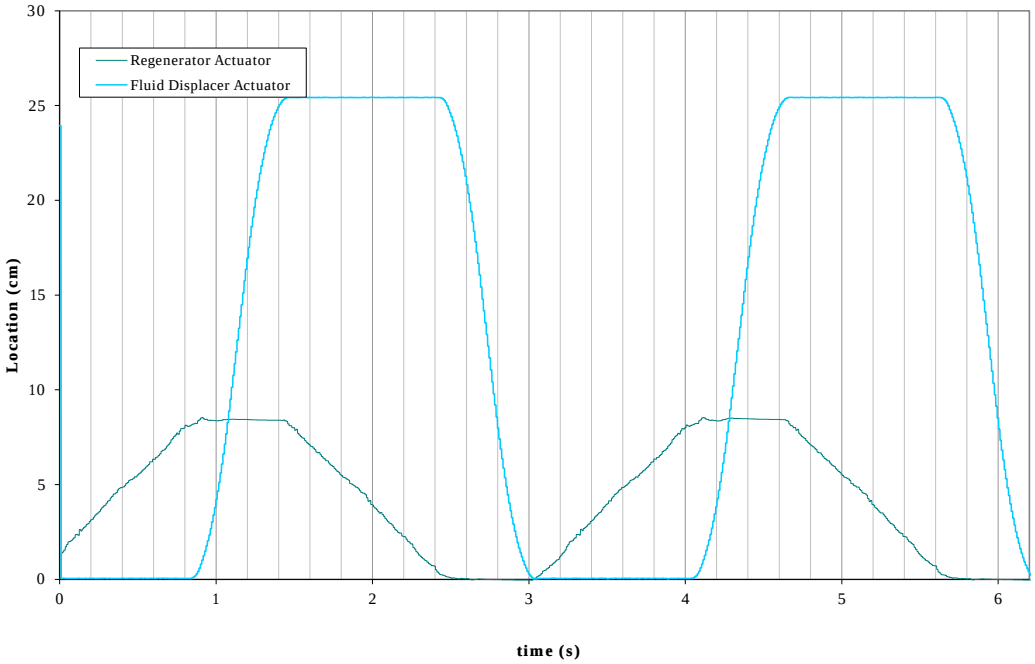

Figure 11. Fluid displacer and regenerator drive motions for the AMRR cycle.

Figure 11 illustrates position as a function of time from the pneumatically-actuated reciprocating drive of the dual magnetic regenerators and the drive motion of the pneumatically actuated positive displacement pump moving the heat transfer fluid (see section 3.8). Note that the two reciprocating motions are trapezoidal in time and out of phase with one another as required to properly execute the AMRR cycle.

3.8. Heat Transfer Fluid System

The magnetic refrigerants in a layered magnetic regenerator are coupled to each other and connected to the heat sink and thermal load from the process stream via a heat transfer fluid (HTF) such as helium gas. The HTF system design incorporated the following criteria:

- uses pressurized helium gas at HTF
- forms closed loop to reciprocating circulation
- contains a by-pass flow control mechanism
- hot heat exchanger rejects heat near 290 K
- is equipped with temperature, flow rate, pressure sensors to determine heat rejected heat.

The HTF subsystem of the 290 K to 120 K AMRL prototype contains three heat exchangers and a chiller, along with several control valves, temperature sensors, and a circulator. We analyzed the heat transfer and pressure drop of several choices for the hot heat exchanger, the cold heat

exchanger between the dual magnetic regenerators, and the bypass flow heat exchanger. This involved investigating the heat transfer surface area needed to cool hydrogen to ~120 K and to remove excess heat from the heat transfer fluid, helium. Helium was selected as the heat transfer fluid based on its ability to transfer heat at cryogenic temperatures and because it is nonflammable and nontoxic.

As the detailed design of the heat transfer fluid subsystem was done, the requirement to have an extremely compact cold heat exchanger and variable bypass flow after the thermal load was added to the cold heat exchanger was extremely challenging. The ability to continuously vary the amount of bypass flow of the heat transfer fluid from zero to as much as ~25 % of total flow through the regenerator caused significant design modifications to the heat transfer fluid subsystem. For example, the cold heat exchanger located between the dual regenerators was eliminated from the subsystem because the external thermal load can be provided from the counter-flowing process stream in the bypass heat exchanger. This change eliminated a complex component and also simplified the design. The revised specifications for the bypass heat exchanger were created.

The helium gas heat transfer fluid subsystem for the AMRR prototype was assembled and tested. Helium gas at ~250 psia was chosen as the HTF after considering using a liquid. We designed this HTF subsystem to be able to provide sufficient He gas flow rate for a wide range of AMRR tests, and especially to be able to exceed the flow rates calculated as optimal in our performance simulation models including bypass flow. The pneumatically actuated mechanical drives for the heat transfer fluid pump worked very well after we figured out how to reduce friction, balance the flow rates in both directions of the piston pump, and eliminate the force imbalance in the piston pump as the mean pressure in the double-acting piston within its cylinder was increased from near atmospheric pressure up to ~250 psia.

The requirements for reciprocating flow during the AMRR operation led to several designs; the simplest was a hermetic pressurized cylinder with a piston displacer that is moved back and forth with a programmable linear actuator controlled by the LabVIEW program. The components of the heat transfer fluid subsystem are shown in Figure 12. Figure 12 illustrates a simplified piping and instrumentation diagram (P&ID) for the HTF subsystem. It can be used to understand the relatively complex reciprocating flows of the heat transfer fluid during the AMRR operation. The helium HTF flows in a reciprocating motion from hot to cold and cold to hot through the dual magnetic regenerators as they are moved in/out of the magnetic field. The chiller insures that T_H is constant during the hot to cold blow period. The cold thermal load HEX between regenerators is not shown although the bypass flow path is illustrated as coming out of the cold region.

The HTF subsystem has a few critical elements which enable us to control and monitor the T, P, and mass flow rate of the inlet and outlet He gas flowing through the regenerators and through the bypass flow loop. There are two brazed plate frame heat exchangers, HX-01 and HX-02, in the flow loop that are connected to a high precision vapor compression cycle chiller with R-404A as its refrigerant. The cold R-404A refrigerant mixture is thermally coupled to the He gas in these two heat exchangers via a circulated mixture of ethylene glycol and water. Using this chiller-heat exchanger combination allows us to precisely control the inlet fluid temperature of the He gas at the hot end of each regenerator at any selected temperature within the range 253-313 K.

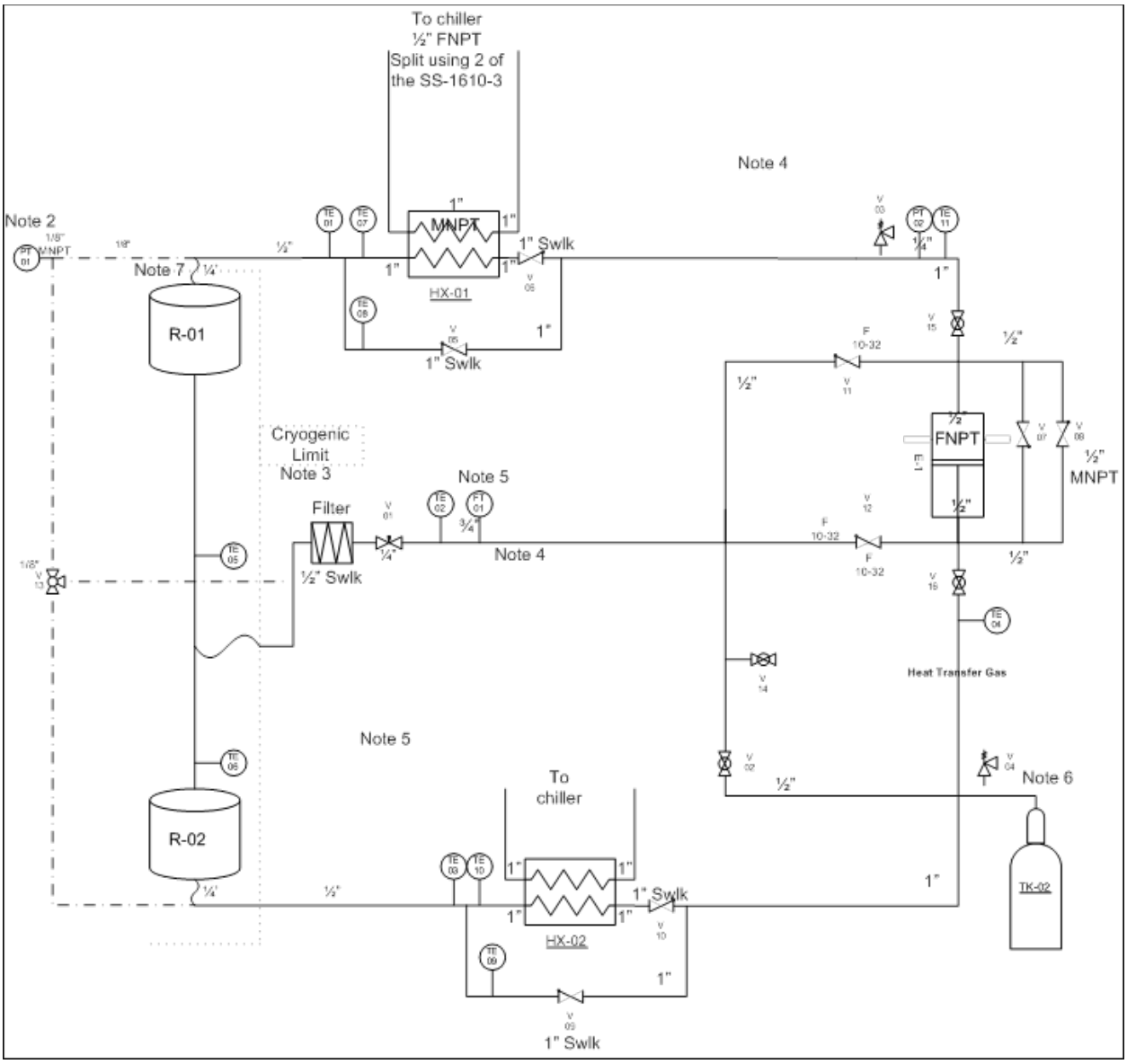

Figure 12. The Heat Transfer Fluid subsystem is illustrated on this simplified P&ID.

A steady He gas hot sink temperature enables precise study of the effect of inlet temperature (T_{hot}) on the cooling power of the AMRR. Figure 13 shows photographs of the heat transfer fluid subsystem components including the brazed plate frame, counter-flow heat exchangers to couple the hot helium heat transfer fluid to the cold refrigerant from the vapor compression cycle chiller used to ensure a stable hot temperature of the heat transfer fluid during an experimental run of the AMRR. The heat exchangers HX-01 and HX-02 are shown well in the top right picture. The reciprocating actuator drive is shown in the bottom right picture. The drive is connected to the double acting piston pump mounted above it. The chiller is located in the center of the top left photograph.

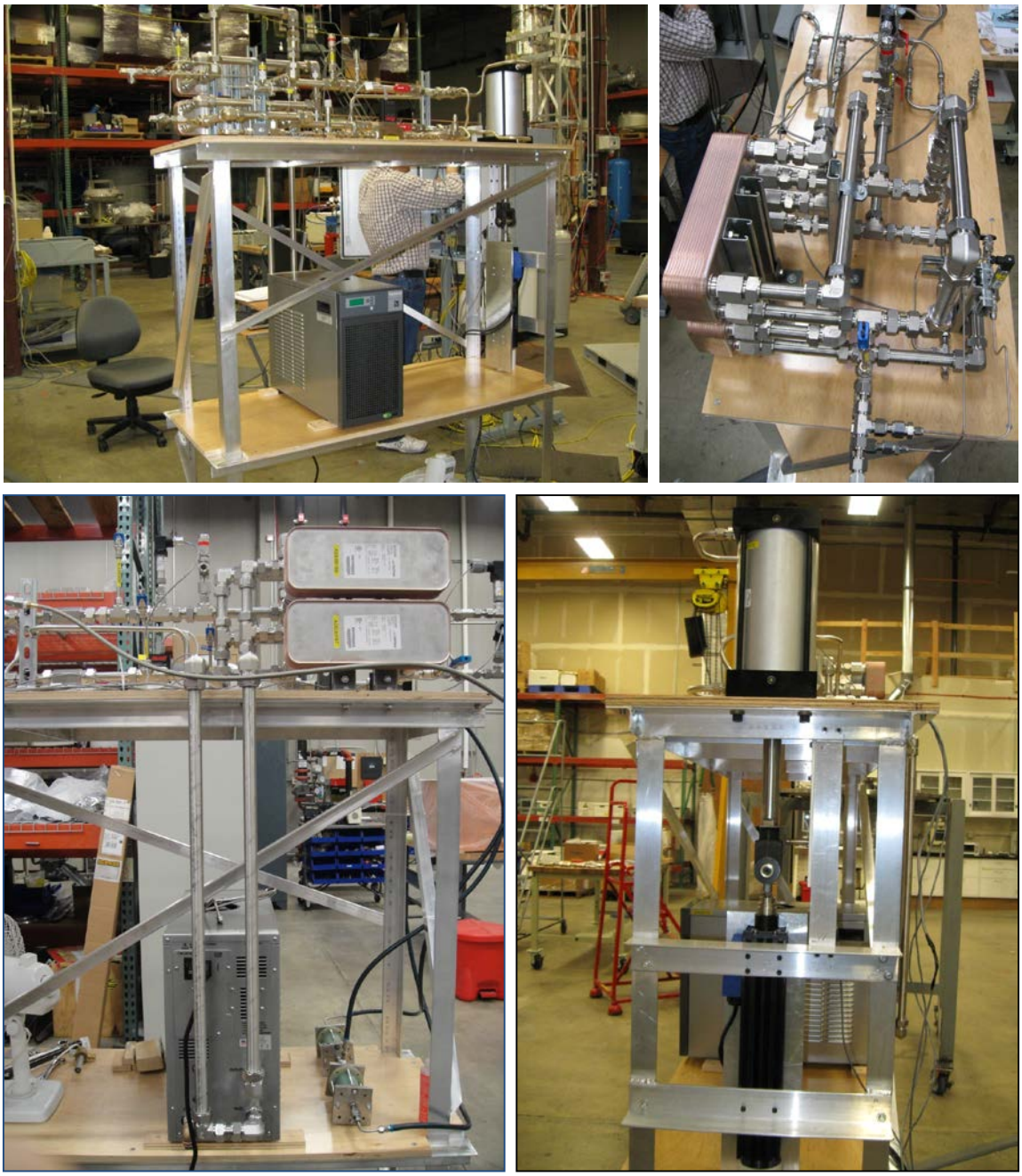

Figure 13. Heat Transfer Fluid (HTF) subsystem components and the AMRR drive actuator (bottom right) with coupling to HTF positive displacement pump. The chiller coupling to HTF circuit (bottom left picture) allows controllable T_H temperature.

The second important independent parameter that we intended to study for the first time is the bypass heat transfer fluid flow rate. Our numerical simulations of the AMRR performance indicates that the thermodynamic efficiency of the magnetic regenerators improves significantly with ~10-15 % bypass flow of the heat transfer fluid during the hot-to-cold blow period of either regenerator. To measure the bypass flow rate and determine its effect on AMRR efficiency, we have installed a precision flow meter in the return flow loop that returns the bypass flows to the

intake portion of the piston pump. We had to add an adjustable valve in bypass flow return lines to closely balance the bypass flows from either magnetic regenerator in different stages of the AMRR cycle.

In addition, we have installed several custom-made high speed ribbon thermocouples to accurately measure the changes in temperature caused by flow reversal during the AMRR cycle. These temperature changes are necessary to calculate the total heat rejected by the system (Q_{hot}) as well as to understand the dynamic temperature profiles of the regenerators. Together, these sensors provide us with good knowledge of important performance parameters from which we can collect precise data for analysis and comparison to expected performance.

The helium flow rate is controlled by a linear actuator (see Figure 14) which moves the double acting piston within a sealed, cylindrical heat transfer fluid container. The fluid actuator and the mechanical drive system actuator are linked to each other so that one is stationary while the other moves. By using electronic linear actuators and a properly programmed LabVIEW control program, we can study different magnetic regenerator motions and fluid flow rates, which can be independently modified if necessary.

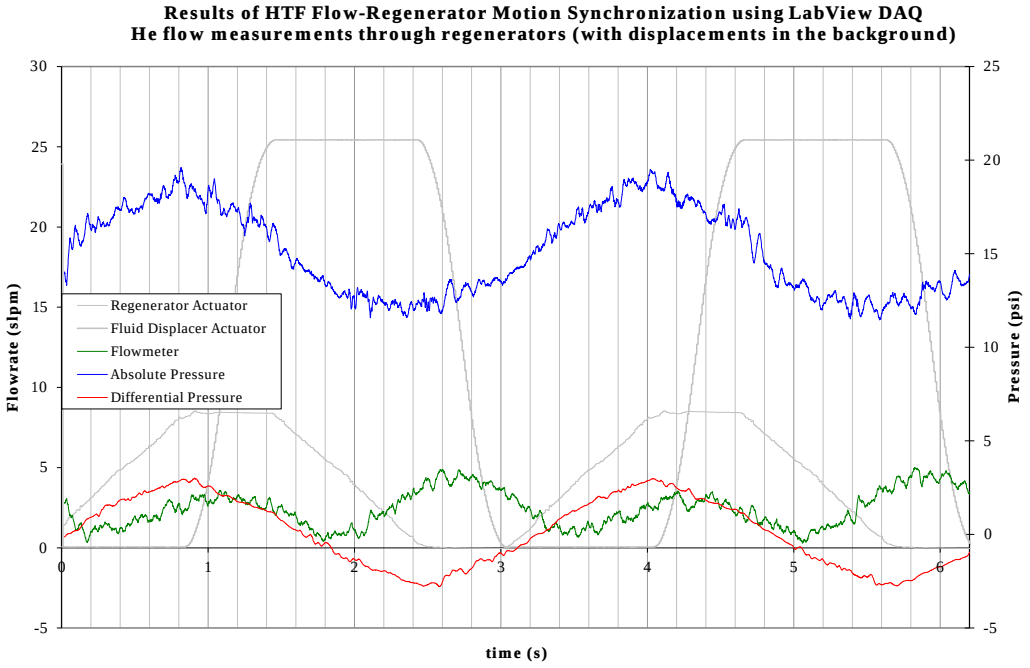

Figure 14. The Heat Transfer Fluid (HTF) flow and regenerator drive motions for the AMRR cycle.

The heat transfer fluid is coupled to the process stream via high performance heat exchangers. The subsystem to supply and circulate the process gas through the AMRR prototype was included in this subtask. The process fluid flow circuit is relatively simple compared to the HTF subsystem. The initial tests were to be done using nitrogen or helium gas as the process stream until the first prototype is fully operational. Several experiments were planned to ensure the counter flowing process heat exchanger is properly specified for use with hydrogen.

4. Preliminary Experimental Test Results

A range of experiments was designed to scope out the AMRR performance. The most significant project results are summarized in bullet form.

- We designed, built, and tested the conductively-cooled superconducting magnet system.
- The GM cryocooler first stage cooled the thermal shield in the cold box to ~45 K and the second stage cooled to below 4 K.
- The vacuum in the cold was an excellent low value of ~1 x 10^{-7} torr when the cryocooler was cold.
- The magnetic field strength reached 4 T. The magnet was tested to 7 T at the vendor's site so this does indicate we have some unidentified heat source that has to be eliminated in the future.
- We completed the design, fabrication, and test of the dual Gd magnetic regenerators, two pneumatic drives, and the heat transfer fluid subsystems of our reciprocating active magnetic regenerative refrigerator (AMRR) prototype.
- The LabVIEW DAQ and control programs have proven to work well during the test runs of the AMRR cycle.
- On our initial AMRR run, the He heat transfer fluid pressure was at 163 psia, the magnetic field at 3 T, a 10 cm stroke in the He reciprocating piston pump, and a 2 second total cycle period, and a variable external thermal load of 0 to 15 W, with a hot sink temperature (T_H set by the chiller) equal to 300 K, we achieved a maximum cold temperature of 253 K or a temperature span across each regenerator of 47 K with zero bypass flow of the He heat transfer fluid. It surpasses previously reported comparable data in the literature by a substantial amount.
- From the curve of the measured value of T_C as a function of external added thermal load, Q_{load}, of 0 W to 15 W, we determined that the parasitic heat load $Q_{parasitic}$ is less than ~5 W. This is a great result given the limited amount of superinsulation that we installed between the 4 K surfaces around the s/c magnet, the 45 K thermal shields, and the thin stainless steel tube in which the much hotter magnetic regenerator subsystems operate.
- The effect of the mass flow rate of the He heat transfer fluid on the temperature span was measured by varying the stroke of the pneumatic drive for the He reciprocating piston pump in the hermetic pump cylinder. The stroke was varied from 2 cm to 8 cm at constant frequency for a 2 second dwell, Q_{load}, and 3 T field. These results clearly indicated that the cooling power increased steadily as the stroke increased, i.e., as the He mass flow rate increases, the cooling power increases and the temperature span increased steadily.
- These He mass flow results show that even with the 10 cm stroke in the He pump for this AMRR cycle frequency, the He mass flow rate is too small to achieve maximum cooling for this AMRR at these operating variables. Given the dimensions of the He reciprocating pump, the best way to increase the He mass flow rate was to increase the mean pressure of the He in the pump cylinder to its design value of ~250 psia and increase the drive stroke to its maximum value of ~20 cm or more. We learned that the first pneumatic drive actuator we selected for the He pump provided insufficient power to execute the trapezoidal-shaped drive motion of the pump required for the AMRR cycle at higher

frequencies, i.e., fast steady movement for uniform He flow, dwell time for no flow, fast steady reverse motion for reverse flow, and the same dwell time for no flow. We found a similar drive with significantly higher power to accomplish the desired He mass flow rates. We purchased this actuator for the He pump but did not have time to install it.

- We experimentally demonstrated the first cooling curves of our AMRR and reached a 50 K span between T_H=295K and T_C=of 245 K.
- We designed experiments to measure AMRR performance under a variety of different operational parameters such as cycle frequency, magnetic field strength, heat transfer fluid flow rate, amount of bypass flow of the heat transfer fluid while measuring work input, temperature span, cooling capability as a function of cold temperature as a function of the amount of bypass flow of the heat transfer fluid for ~290 K to ~240 K temperature span.
- Everything we have learned so far from the reciprocating AMRR prototype is driving us strongly toward a rotary magnetic wheel design of the next AMRL prototype.
- The use of bypass flow (see Figure 15) of heat transfer fluid (He in Figure 15) in an AMRR should give two big improvements; reduction of temperature approach in process heat exchanger and eliminates intrinsic irreversibility of magnetic refrigerant. We expect that ~15% of bypass flow should significantly improve the thermodynamic performance. Due to the limitations of the installed He pump we did not carry out bypass experiments yet.

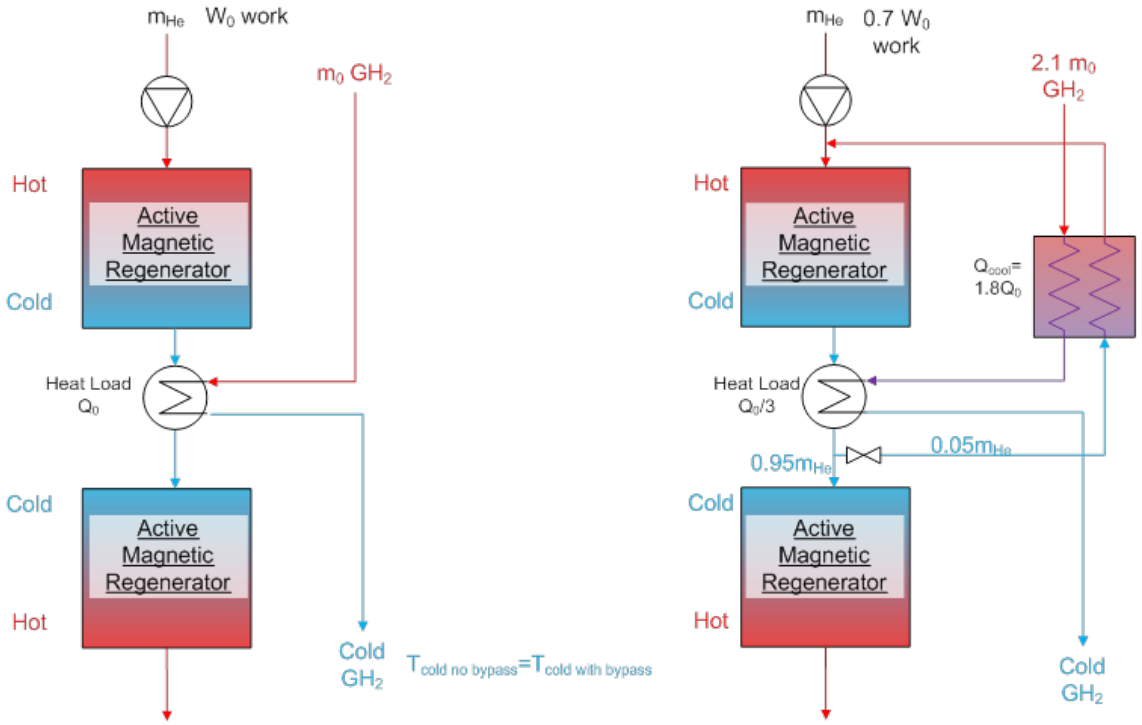

Figure 15. Schematic Representation of the Bypass Concept.

5. Project Management and Reporting

Throughout the project interim progress reports and other deliverables were e provided in accordance with the Federal Assistance Reporting Checklist following the instructions included therein. Participation in DOE's annual Hydrogen Merit Review Meetings and other relevant meetings to present progress on this project was anticipated as part of this task.

6. Cost Status

The last financial report sf-425 was submitted in January 2013. Prometheus did not accrue any additional project expenses since January 2013 until the project was canceled and during the AMRL equipment transfer to PNNL.

7. Description of any product produced or technology transfer activities

No invention disclosures or patent applications were made during the project.
Prometheus created a digital database of scientific articles and publications pertaining to magnetic refrigeration and liquefaction.